Research Article

Investigation on the Corrosion Inhibition Behaviour of Polymer-Rice Husk Composite on Mild Steel Surface in 1M H_2SO_4

PR Sivakumar*

Department of Chemistry, Adithya Institute of Technology, Coimbatore-641 104, Tamil Nadu, India

Abstract

Composites have gained significant attention in recent years as a potential structural material. Rice husk and ceramic composites are an important area of interest for the development of (investigations on polymer-based composite materials have opened) new routes for polymer formulations (composite materials), as their industrial applications are low cost, light weight, high specific modulus, renewability (non-carcinogenic), and bio degradability. Keeping this in mind, the current study aims to investigate the use of rice husk as a potential filler in polymer composites and to investigate its corrosion behavior. Weight loss, EIS and Tafel polarization were used to assess the corrosion protection of a prepared polyester rice husk composite on mild steel in 1M sulphuric acid. At higher inhibitor concentrations, the polymer composite's optimum inhibition efficiency reached 97%. SEM, EDS, XRD, and AFM were used to investigate the surface morphology of mild steel with and without inhibitor. FT-IR, TGA, XRD, SEM, and EDS were used to confirm the formation of the polymer composite (polymer-rive husk).

Keywords: composite, corrosion inhibitor, mild steel, Tafel slopes, EIS, SEM, XRD, AFM

***Correspondence**

Author: PR Sivakumar

Email: shivarashee@gmail.com

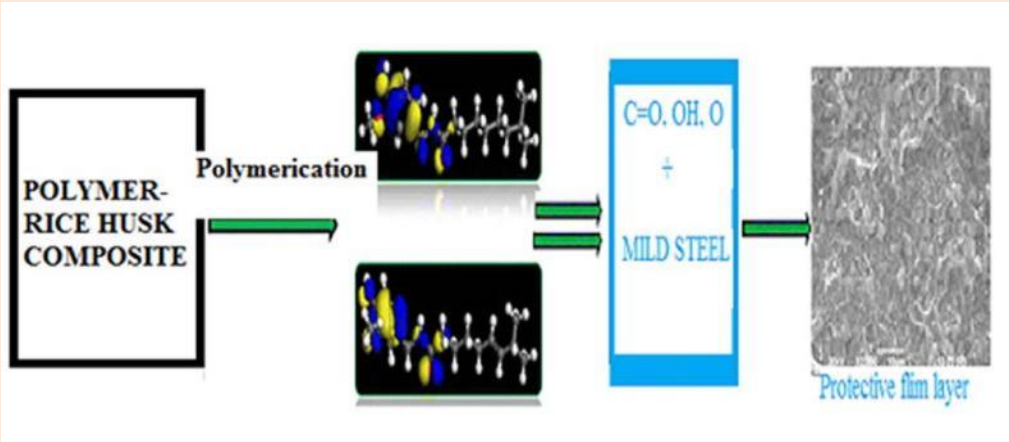

Introduction

One of the world's current challenges is determining how to manage and prevent metal corrosion [1]. There are several control techniques for protecting mild steel from corrosion in corrosive environments. Synthesis or natural or organic inhibitors have been developed and used on a regular basis, taking into account. It is one of the least expensive inhibitors for preventing metal corrosion. Several researchers have suggested that certain plant extracts can be used as corrosion inhibitors [2]. The disposal of rice husk is a particularly serious issue that necessitates special attention due to its large quantity [3-5]. In terms of organic fillers, rice husk (approximately 20%), a widely available agro-waste byproduct [6-7] obtained from the milling process of rice (Oryza sativa), one of the world's major food crops, can be used as material properties [8-10]. Because of its stiffness, strength, and ease of use. Increased environmental awareness has led to the development of methods for the effective utilization of rice by-products, particularly rice husk, which is valuable due to its high content of amorphous silica. Rice husk contains approximately 35% cellulose, 35% hemicellulose, and 20% lignin and ash (10% of which silica is 94%). Ash has a typical composition of 95% SiO_2, 2% K_2O, 1% CaO, P_2O_5 and Na_2O_3, Fe_2O_3, MgO, and standard lingocelllosic material, with lower lignin and hemi cellulosic contents than wood flour [11-13]. Many researchers have emphasised the fact that

the rate of increase in the active surface area increases when the material is attached [14-16]. To the best of our knowledge, no reports on the use of polyester rice husk composite as anticorrosive materials have been published. The purpose of this work is to investigate the effect of a polyester-rice husk composite as a mild steel corrosion inhibitor in 1M H_2SO_4.

Experimental

Synthesis of polymer composite

Polyester composite was synthesized from polyester containing oxadiazole unit and rice husk [Scheme 1].

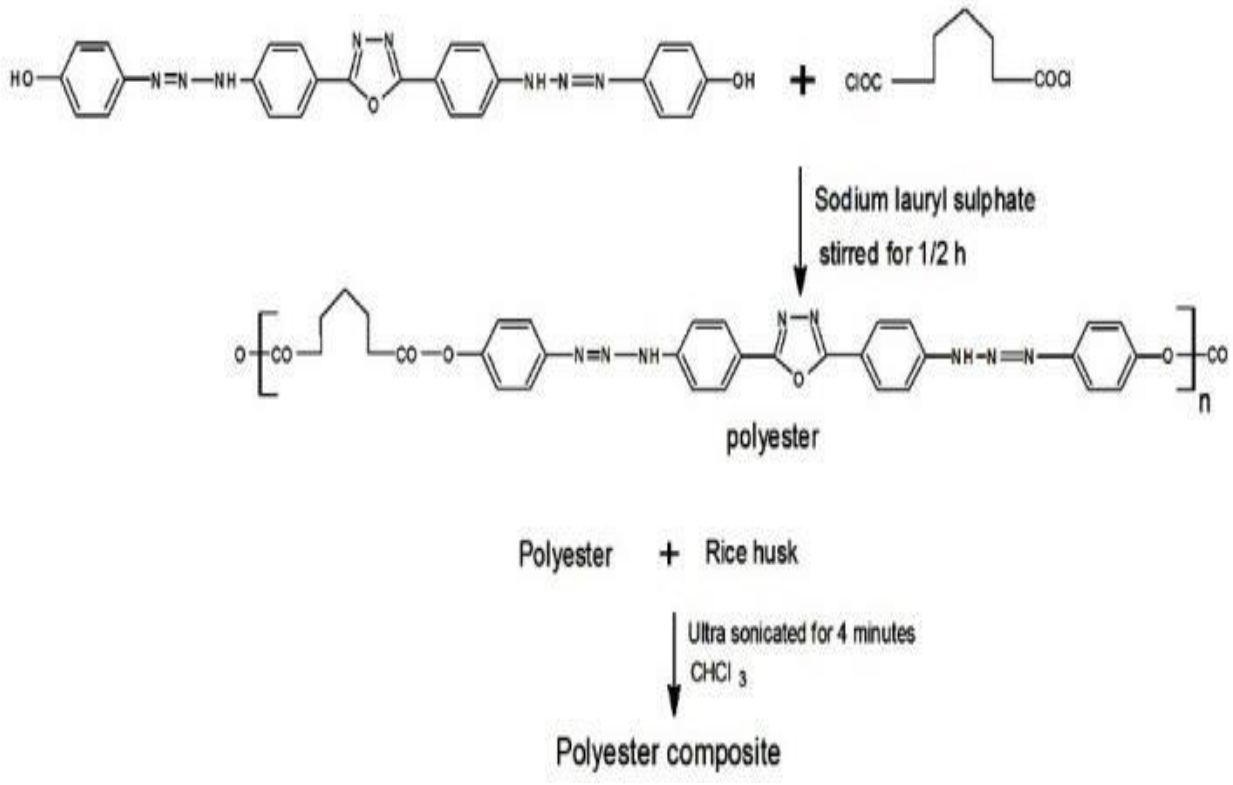

Scheme 1

Synthesis of polyester

The monomer oxadiazole (2,5-bis(4-aminophenyl)-1,3,4-oxadiazole) was polycondensed with pimelic diacid chloride (14.6g of crystallised pimelic acid was refluxed in an oil bath for about 4 hours with 27ml of distilled thionyl chloride). In a 1:2 mole ratio, one equivalent of the monomer was stirred with aqueous sodium hydroxide until a clear solution was obtained. To this, 0.05g of sodium lauryl sulphate was added and blended for 30 minutes in a high-speed blender. The diacid chloride equivalent was quickly added in a minimum volume of freshly distilled chloroform. The reaction mixture was then vigorously stirred for 20 minutes before being poured into acetone to coagulate the polymer. The precipitated polymer was filtered and washed with water, dilute sodium carbonate solution, and acetone several times [17-19].

Synthesis of polyester composite

Preparation of rice husk for composite formation

Step 1: Surface modification of cellulosic fibres entailed removing impurities from the fibre surface in order to improve its physical and chemical properties. Sodium hydroxide removes (impurities) natural fats and waxes from the surface of cellulosic fibres (improves fiber-matrix interface bonding), exposing chemically reactive functional groups such as –OH (hydroxyl) and other reactive functional groups. The removal of surface impurities from cellulose fibre improves the surface roughness of the fibres [20]. Rice husk was soaked in a 0.5N NaOH solution at room temperature in a ratio of 500ml alkali solution/50g rice husk and immersed in the alkali solution for 2 hours. The fibres were then rinsed multiple times with distilled water before being dried and utilized to make the composite.

Step 2: Polyester (500ppm) was added to 10 ml of chloroform, and a sufficient amount of alkali treated rice husk (100ppm / 300ppm / 500ppm) was completely dispersed into the solution using a quick ultra-sonication for 4 minutes to accelerate rice husk dispersion. The ultrasonically processed materials were dried and employed as inhibitors [21-22]. The inhibitor concentration was measured in parts per million (ppm) for further study. The produced polyester composites were classified using FT-IR, TGA, and XRD, and their morphology was scanned using SEM-EDS.

Materials and Method

Mild steel specimens, electrodes and solutions

The chemical composition by weight of mild steel is 0.084 % C, 0.369 % Mn, 0.129 % Si, 0.025 % P, 0.027 % S, 0.022 % Cr, and 0.011 % Mo, 0.013 % Ni, and balance iron. For the investigation, mild steel coupons with dimensions of 3cm x 1cm x 0.1cm were utilized for weight loss measurements, and mild steel rod with an exposed area of $1cm^2$ was used for electrochemical tests. IR spectra taken with a Shimadzu IR Affinity 1 spectrometer validated the structure of the manufactured polyester composite. The thermo grams were recorded using a Perkin Elmer (TGS-2 model) thermal analyzer in a dynamic nitrogen environment at a heating rate of 10 C. Wide angle XRD employing Brucker XRD at STIC, CUSAT, Cochin was used to evaluate the percentage of crystallinity in the produced polymer and its composites. The surface morphology was captured using an EDS detector in conjunction with a SEM on a Medzer biomedical research microscope (Mumbai, India). IVIUM Compactstat Potentiostat / Galvanostat software was used to do the electrochemical experiments.

Results and Discussion

IR spectral studies

Figure 1 compares the FT-IR spectrums of polyester, rice husk, polyester rice husk composite, and mild steel surface (without and with inhibitor). The IR spectra of polyester (Figure1a) contains bands at $3020cm^{-1}$, $1679cm^{-1}$, $1600cm^{-1}$, and $1078cm^{-1}$, which are indicative of the -NH, >C=O, C=N, and C-O-C groups. The IR spectra of alkali-treated rice husk (Figure 1b) shows bands at $3300cm^{-1}$, $2925cm^{-1}$, $1748cm^{-1}$, and $1510cm^{-1}$ that have been ascribed to the stretching frequencies of hydroxyl, >CH stretching, carbonyl, and >C=N / C=C groups. These bands may also be attributed to active elements of rice husk, such as hemicellulose esters and carboxylic groups, lignin aromatic rings, alkane, alkenes, and nitrogen-containing compounds. The IR spectrum of the composite (Figure 1c) and (Figure 1d exhibits the merged FT-IR spectra of the composite and the metal surface) demonstrate that their molecules include identical types of functional groups. As shown in Figure 1d, the adsorption of the polyester composite (PES-RH) onto the mild steel surface has been coordinated.

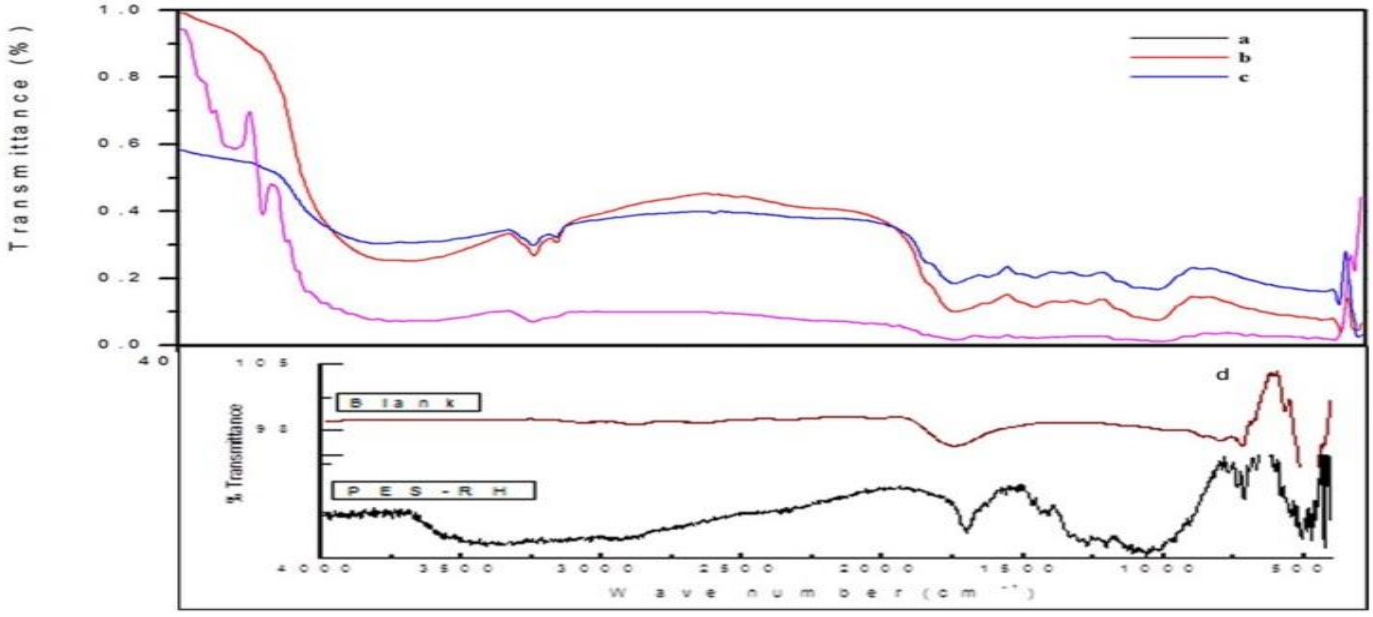

Figure 1 (a) FT-IR spectrum of polyester (PES), (b) FT-IR spectrum of RH, (c) FT-IR spectrum of PSE-RH, (d) mild steel plate, (e) FT-IR spectrum of polyester and immersed in the presence and absence of the inhibitor in 1M H_2SO_4.

Thermal studies

Figure 2 depicts the TGA results of polyester, alkali-treated rice husk, and polyester composite (a, b & c). The thermal deterioration of polyester (Figure 2a) occurs in a single step around 270-320 C, which may be attributed to the major pyrolitic rupture of -N=N, with the evolution of aromatics beginning at around 300 C with the breakdown of the oxadiazole backbone. Figure 2b shows the results of the thermal study of rice husk. Degradation happens in two stages, 270-330^{o} C and 330-650^{o} C. (Figure 2b). The first and second temperature transitions correspond to cellulose/hemicellulose and lignin thermal breakdown temperatures, respectively. The initial degradation temperature shows in the temperature range 260-340^{o} C in the TGA of rice husk-filled polyester (Figure 2c). The result implies that cellulose and hemicellulose components in rice husk have degraded [23]. Furthermore, the second temperature degradation is detected in the 350-500^{o} C range due to lignin and polyester PES components. The thermal stability of the polymer composite is intermediate between the thermal stability of the polymer PES and the thermal stability of the filler RH material.

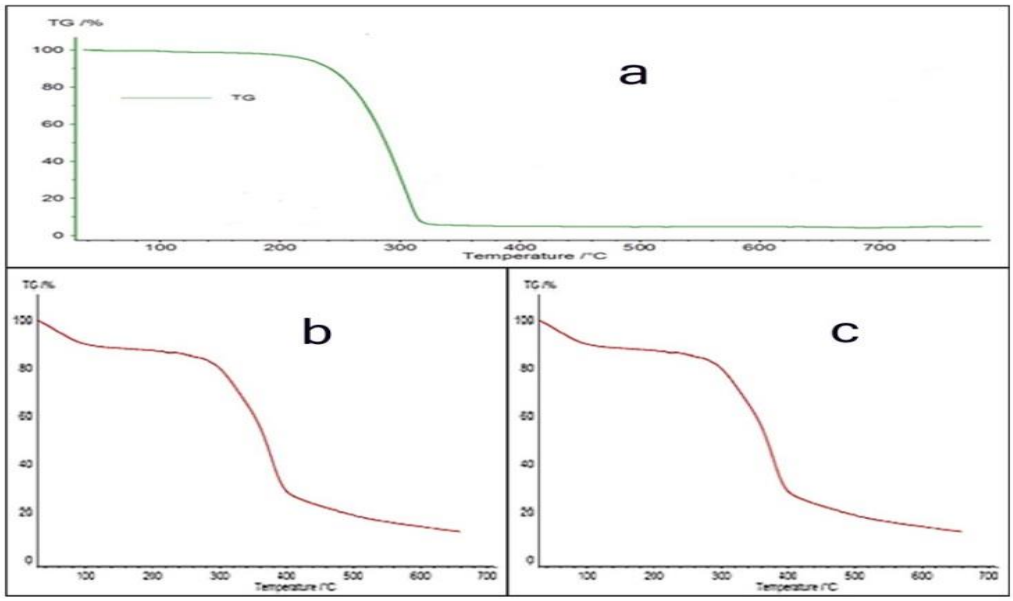

Figure 2 (a) Thermogram of PES, (b) Thermogram of PES, (c) Thermogram of PES

XRD Studies: polymer composites

Figure 3 depicts X-ray diffraction patterns of rice husk, polyester, polyester composite, and mild steel surfaces. The rice husk's XRD pattern (Figure 3a) indicates that it is amorphous, whereas the polyester is crystalline. The addition of the filler material to the polymer matrix in the composite results in the elimination of peaks, confirming the semi-crystalline character of the material and the development of the composite. The XRD analysis for the surface of mild steel immersed in 1M H_2SO_4 with and without inhibitors is shown in Figure 3b. The roughness of the substrate's surface causes disturbances in the X-ray pattern. The XRD pattern of mild steel in blank solution exhibits iron peaks at 2θ = 28.2°, 35.3°, and 62.1°. The X-ray diffraction pattern of polyester composite (PES-RH) reveals iron oxide peaks at 2θ = 44.58°, 64.86°, and 82.25°. As a result, the surface of the metal immersed in acid media contains iron oxides, most likely Fe_3O_4 and FeOOH [24-26]. The protection of the mild steel surface by polyester composite has been confirmed (PES-RH).

SEM studies

SEM images revealed some interesting morphological changes between rice husk, polymer, and polymer composite. The surface of the rice husk has been considerably roughened, resulting in linear ridged structures, as seen in Figure 4b. The porous nature and rough surface of the polymer, on the other hand, are clearly visible in the SEM picture in **Figure 4a**. As seen in Figure 4c, the surface of the polymer composite is flaky. Polymer composite has a different surface morphology than rice husk and polymer. The surface of the modified polymer composites shows good progressive changes in the SEM pictures. SEM micrographs of the mild steel surface in 1M H_2SO_4 solution (Figure 4d) show the changes that occurred during the corrosion process in the absence and presence of inhibitor. The mild steel surface was more damaged in 1 M H_2SO_4 than in the presence of (500ppm polyester+500ppm rice husk)

polyester composite (PES-RH), although the surface was much improved and less damage (shows smoother) happened when compared to their surfaces in the absence of inhibitors. It denotes the creation of a passive layer (protective film) on the metal surface (improvement in surface morphology) by which the corrosion rate lowers in the presence of an inhibitor (responsible for inhibition) and the electrochemical reaction is diminished [27].

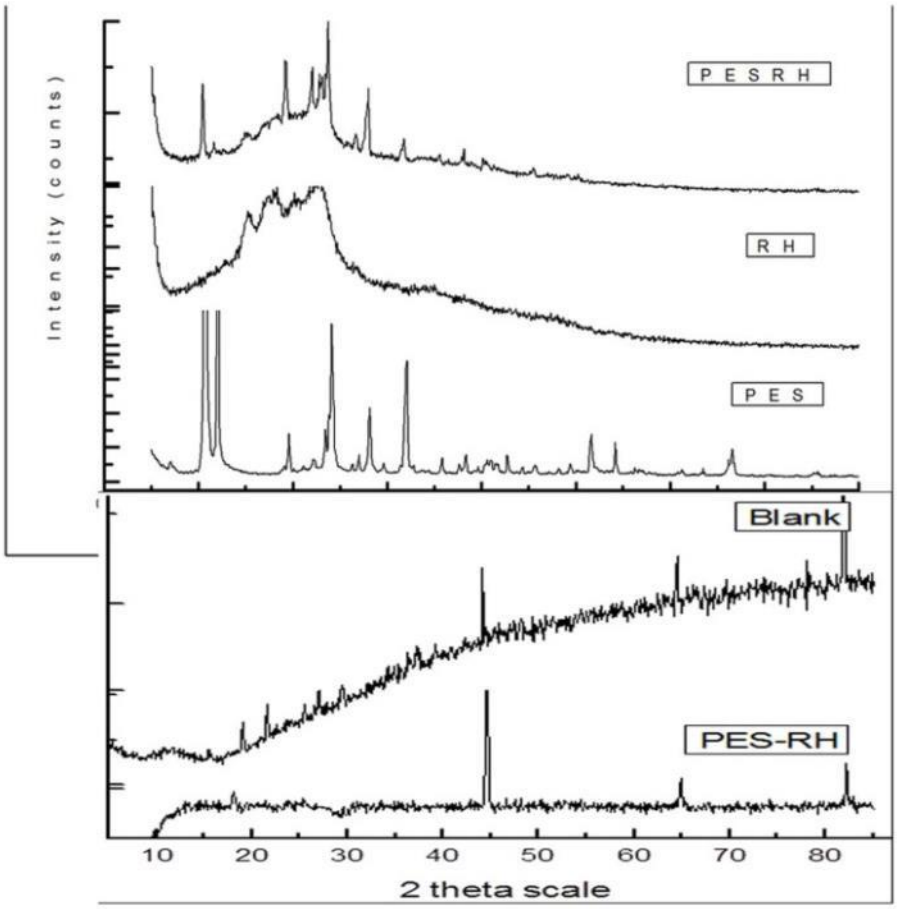

Figure 3 a XRD pattern of PES–RH and XRD pattern of mild steel surface in the presence and absence of inhibitor in 1M H_2SO_4

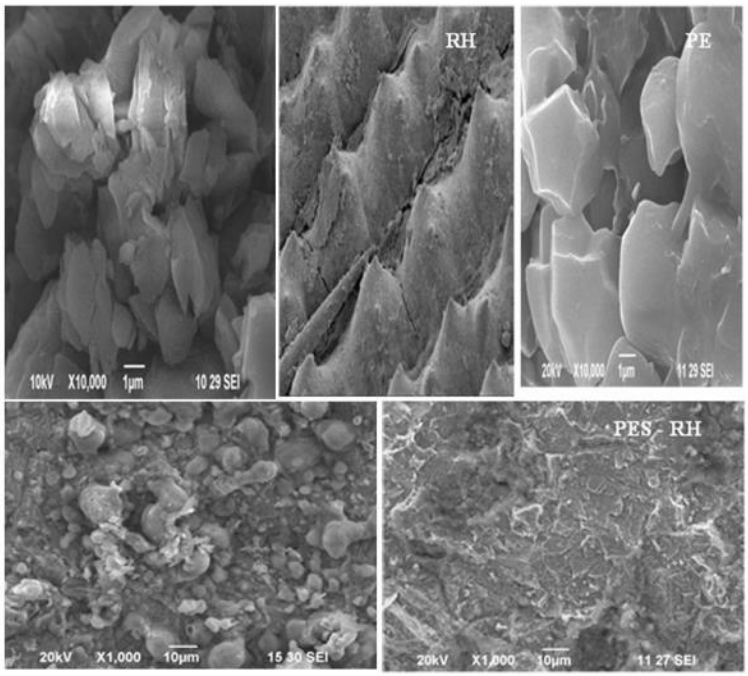

Figure 4 Scanning electron microscopic image of polyester (PES) and photographs of mild steel plates in the absence and presence of the inhibitor

EDS STUDY

As shown in **Figure 5a, b** and **Table 1**, an EDS microanalysis of all spectra in the polyester composite reveals the presence of carbon, oxygen, nitrogen, silicon, and calcium, among other elements. This observation has validated the composite's successful creation. Figure 5a depicts the features peak of the components forming mild steel in the absence of inhibitors and the presence of polyester composite (PES-RH), whereas Figure 5b depicts an extra peak due to the presence of C, N, Cl, Si, and O. The components on the maximal surface clearly indicate that the polymer composites included in the inhibitor molecule, such as C, N, Si, O, and Cl, can bond with metal ions via very strong adsorption to protect it from corrosive environments [28].

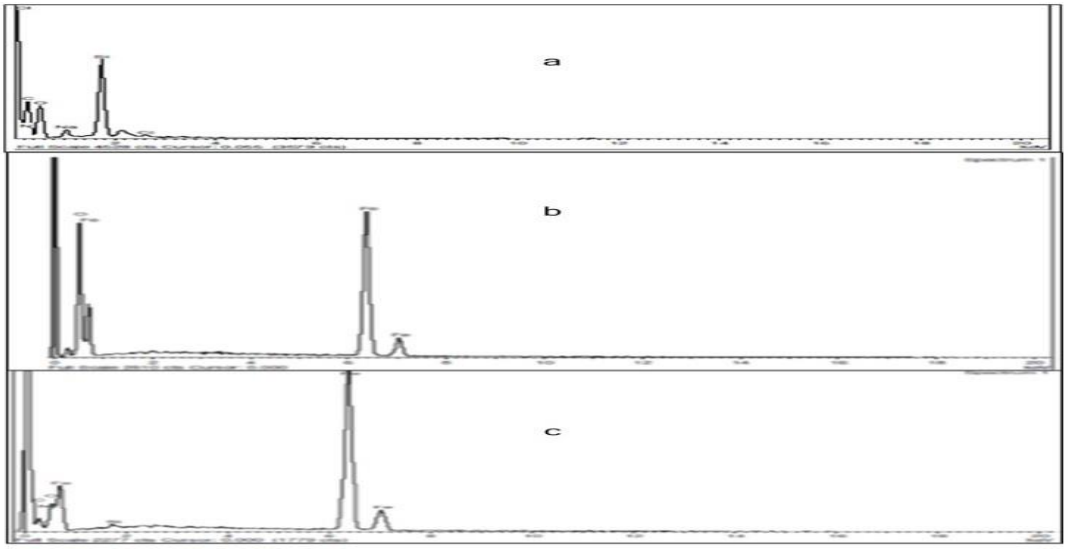

Figure 5 SEM-EDS image of PES-RH a. EDS for Blank (1M H_2SO_4) & b. EDS for PES-RH + 1M H_2SO_4

Table 1 Surface compositions (weight %) of polyester composite of mild steel after 3 hours of immersion in 1M H_2SO_4 without and with inhibitor

Name	**% Mass of polyester composite**						
	Fe	**C**	**N**	**O**	**Si**	**S**	**Na**
PES-RH	-	50.51	0.36	35.72	11.46	-	1.94
	% Mass of mild steel surface						
Blank	66.20	-	-	33.80	-	-	-
MS+PES-RH	58.56	15.91	10.08	15.02	0.43		-

Weight loss method

As shown in **Table 2**, the mass loss method is a non-electrochemical methodology for determining corrosion rates and inhibition efficiency. It depicts the quantitative weight loss measurement profile of pure polyester (PES), pure filler material (RH), and polyester composites (PES-RH) subjected to the mild steel corrosion process in 1M H_2SO_4 medium. The data clearly reveal that PES has a 38.6 % inhibition efficiency at 500ppm while RH has a 58 % inhibition efficiency at the same dose. However, when the concentration of the filler material increases in composites (PES-RH), the inhibition efficiency increases up to 97 % (corrosion rate lowers). They propose a mechanism for production based on the adsorption of molecules from the PES-RH composite. The fact that the maximum IE percent is measured at higher inhibitor concentrations indicates that more inhibitor molecules are adsorbed on the MS surface, providing more surface coverage for the active areas of MS where direct and migrate to protect from corrosion attack [29].

Temperature studies and Adsorption isotherm

Weight loss experiments were conducted at fixed concentrations of inhibitor and aggressive medium at various temperatures (313K, 323K, and 333K) in the temperature studies, and the results are shown in **Table 3**. **Table 4** present the thermodynamic parameters (Ea, $\Delta G°_{ads}$, $\Delta H°_{ads}$ and $\Delta S°_{ads}$)) derived from the data. The activation parameters are crucial in understanding the inhibitors' inhibitive mechanism [30]. **Figure 6a** shows Arrhenius plots of

the logarithm of corrosion rate versus 1/T. The analysis of the results shown in Tables 3 and 4 shows that the inhibition efficiency decreases with increasing temperature. E_a values for polyester (PES) and polyester composite PES-RH were 46.22 kJ/mol and 98.85 kJ/mol, respectively [31]. According to some researchers, the apparent activation energy E_a in inhibited solutions is greater than that in uninhibited solutions because the inhibitors participate in dominating physisorption and inhibition efficacy reduces with temperature increase [32]. In an attempt to determine the activation enthalpy ΔH^o and activation entropy ΔS^o. Figure 6b [33] shows the log corrosion rate/T and 1/T graphs. Table 4 shows that the ΔH^o values for mild steel dissolving in 1M H_2SO_4 in the presence of inhibitors are higher (43.58 to 96.21 kJ/mol) than in the absence of inhibitors (34.72 kJ/mol) [34]. The positive value of ΔH^0 represented the mild steel dissolving process's endothermic nature, implying that mild steel dissolution is difficult in the presence of inhibitors [35]. The values of ΔS^o (which are less negative in the presence of PES and polyester composite) clearly show that the entropy of activation is lower in the presence of the inhibitors investigated than in the absence of the free acid. In the presence of a polyester composite, the low value of ΔS^o favours slower metal dissolution [36]. The findings of this study are consistent with the findings of other researchers [37].

Table 2 Inhibition efficiencies at polyester / polyester composite for corrosion of mild steel in 1M H_2SO_4 from weight loss measurement at 303±1K

Name of the inhibitors	Conc. of PES (ppm)	Weight of filler materials (ppm)	Weight loss (g)	Inhibition efficiency (%)	Degree of surface coverage (Θ)	Corrosion rate ($gcm^{-2}h^{-1}$)
Blank	-	-	0.2209	-	-	14.31
PES	500	-	0.1356	38.6	0.3862	8.78
RH	-	500	0.0936	57.63	0.5763	6.06
PES-RH	500	RH – 100	0.0420	80.99	0.8099	2.72
		RH – 300	0.0122	94.48	0.9448	0.79
		RH – 500	0.0070	96.83	0.9683	0.45

Table 3 Inhibition efficiencies of polyester / polyester composite for corrosion of mild steel in 1M H_2SO_4 from weight loss measurement at higher temperature

Name of the inhibitors	Temperature (K)	Weight loss (g)	Inhibition efficiency (%)	Corrosion rate ($gcm^{-2}h^{-1}$)
Blank	303	0.0736	-	14.31
	313	0.1350	-	26.24
	323	0.1979	-	38.46
	333	0.2846	-	55.31
PES (500ppm)	303	0.0452	38.58	8.79
	313	0.0956	29.19	18.58
	323	0.1533	22.53	29.80
	333	0.2410	15.11	46.96
PES+RH (500ppm +500ppm)	303	0.0023	96.83	0.45
	313	0.0150	88.89	2.92
	323	0.0426	78.47	8.28
	333	0.0805	71.71	15.64

At the metal-solution contact, the solvent (H_2O) molecules have already been adsorbed. The adsorption behavior or mode of adsorption of the inhibitor on the metal surface must be known in order to understand the process of corrosion inhibition. The experimental data were examined using multiple adsorption isotherms to learn more about the manner of adsorption of the inhibitors, PES and PES-RH, on a mild steel surface at room temperature. Attempts were made in this work to fit the values (θ) to several isotherms such as Langmuir, Temkin, Frumkin, and Flory-Huggins. The plot (straight line) of C/θ against C at 303K is shown in Figure 6. The Langmuir isotherm provided by far the best fit. The linearity of the Langmuir plot reveals that the inhibitor molecules adsorb to form a monolayer on the mild steel surface and that there is no interaction between the adsorbed inhibitor molecules [38].

In our measurements, the values of ΔG^0_{ads} (Table 4) ranged from -36.18 to -25.52 kJ/mol. In Figure 6c, the thermodynamic parameters are enthalpy and entropy of adsorption log K_{ads} Vs 1/T. Figure 6d shows a plot of ΔG°_{ads}/T Vs 1000/T. In Figure 6e, a plot of ΔG°_{ads} Vs T was linear. In our work, ΔH°_{ads} values range from -34.21 to 70.10 $kJmol^{-1}$, and ΔS°_{ads} values range from -0.0258 to -0.1138 kJ/mol/K, with the negative sign indicating (spontaneity of the process) that adsorption is accompanied by a drop in entropy [39]. Thus, the physisorption process of polyester

(PES) and polyester composite (PES-RH) adsorption on mild steel in 1M H_2SO_4, as is the stability of the adsorbed layer on the mild steel surface.

Table 4 Activation parameters of mild steel corrosion in 1M H_2SO_4 for polyester / polyester composite calculated by Free energy, Arrhenius, transition state and basic thermodynamic equations

Name of the inhibitors	**E_a (kJ/mol)**	**ΔG°_{ads} (kJ/mol)**				**ΔH° (kJ/mol)**	**$-\Delta S^\circ$ (kJ/mol/K)**
		303 K	**313 K**	**323 K**	**333 K**		
Blank	37.36	67.42	68.50	69.58	70.65	34.72	0.1079
PES (500ppm)	46.22	68.61	69.44	70.27	71.09	43.58	0.0826
PES-RH (500ppm+ 500ppm)	98.85	75.58	74.90	74.22	73.54	96.21	-0.0681
Name of the inhibitors		$-\Delta G^\circ_{ads}$(kJ/mol)					
		303 K		313 K		323 K	333 K
PES (500ppm)		26.35		26.13		26.03	25.52
PES-RH (500ppm+500ppm)		36.18		33.85		32.82	32.83
Name of the inhibitors		Van't Hoff equation		Gibbs Helmholtz equation		Basic thermodynamic equation	
		$-\Delta H^0$ kJ/mol	$-\Delta S^0$ kJ/mol/K	$-\Delta H^0$ kJ/mol		$-\Delta H^0$ kJ/mol	$-\Delta S^0$ kJ/mol/K
PES (500ppm)		34.21	0.0258	34.21		34.32	0.0262
PES-RH (500ppm+500ppm)		70.10	0.1138	70.10		69.16	0.1108

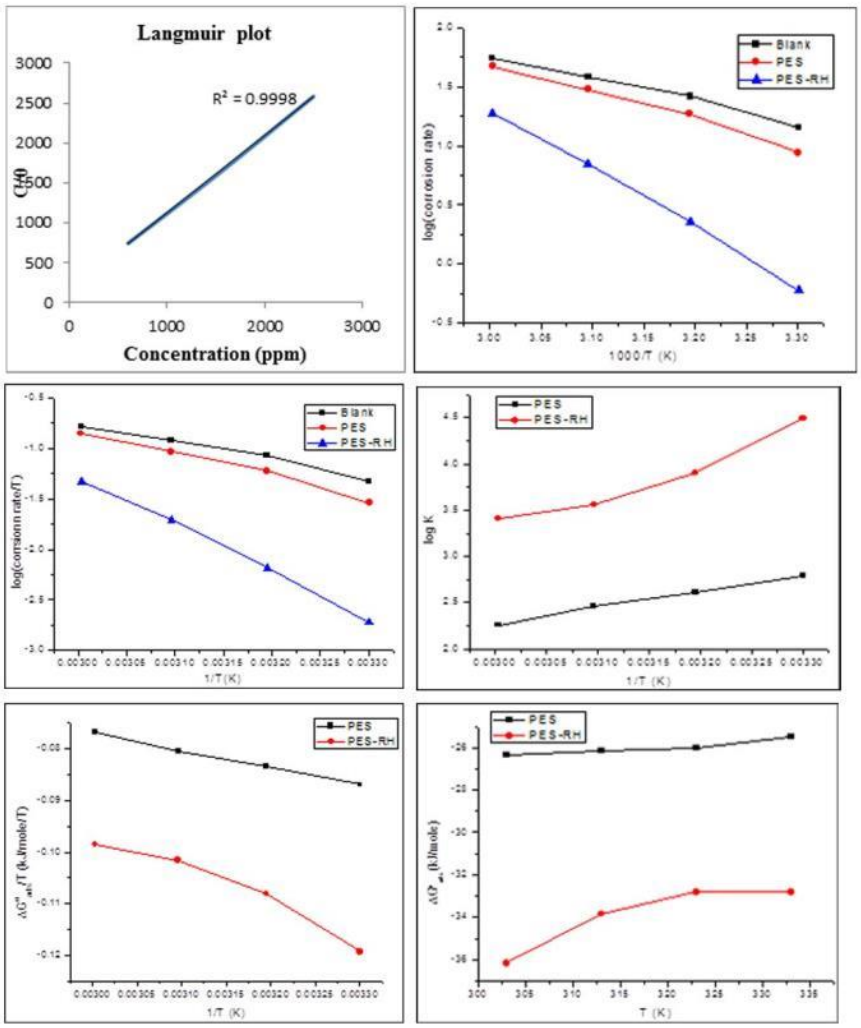

Figure 6 (a) Langmuir plot (b)Arrhenius plot (c) Transition plot (d) The relationship between log K_{ads} and 1/T (e) The relationship between ΔG°_{ads}/T and 1/T, (f) The relationship between ΔG°_{ads} and T plot in 1M H_2SO_4 of corrosion of mild steel in 1M H_2SO_4 solution in the absence and presence of inhibitor

Polarization studies

Potentiodynamic polarisation curves were produced from -200mV to +200mV (against OCP) at a scan rate of 1 mV/s, allowing for the analysis of anticorrosion behavior via anodic and cathodic polarizations. **Table 5** lists the various electrochemical parameters computed from Tafel graphs in **Figure 7**. The decreased corrosion current density (I_{corr}) suggests that the PES-RH composite was successful in suppressing corrosion from both metal dissolving and hydrogen evolution on the anodic and cathodic processes, respectively. It is clear that the compound functions as a mixed-type inhibitor [40].

Table 5 Corrosion parameters of polyester / polyester composite for corrosion of mild steel in 1M H_2SO_4 by potentiodynamic polarization method

Name of the inhibitors	Conc. of PES	Weight of filler materials	Tafel slopes (mV/dec)		E_{corr} (mV)	I_{corr} (μAmp/cm^2)	Inhibition efficiency (%)
			b_a	b_c			
Blank	-	-	52	112	-467.4	1569	-
PES	500ppm	-	34	177	-451.3	990	36.9
PES-RH	500ppm	RH- 100ppm	76	118	-506	1234	21.4
		RH- 300ppm	73	117	-509	1010	35.6
		RH- 500ppm	66	106	-514	821	47.7

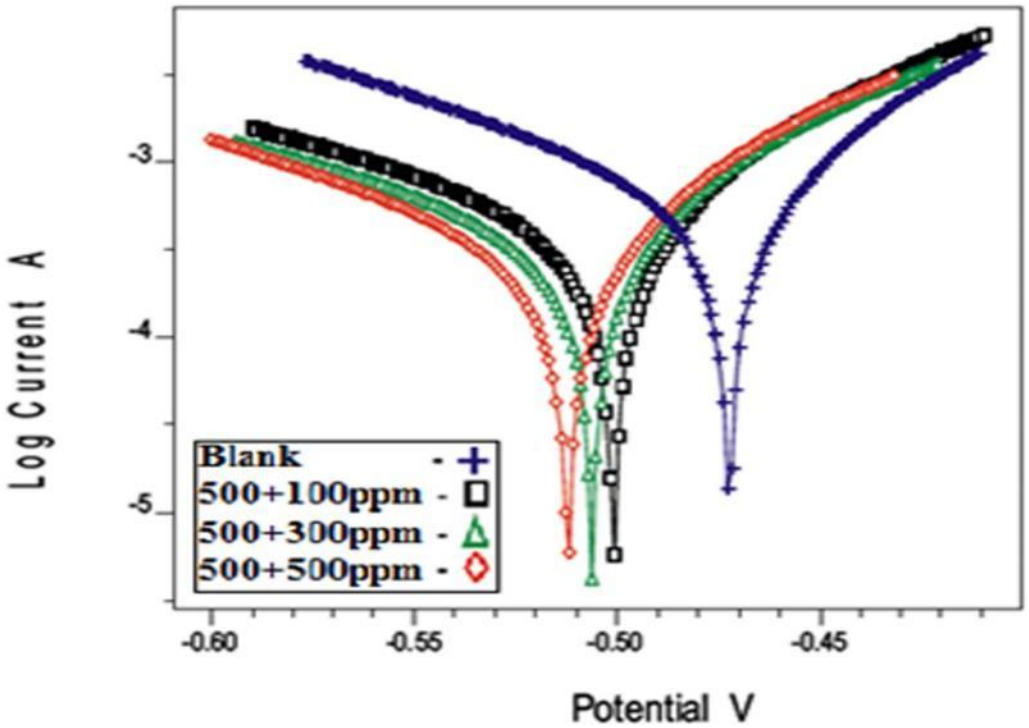

Figure 7 Polarization curves for mild steel recorded in 1M H_2SO_4 for selected concentrations of the inhibitor PES-RH

Electrochemical impedance spectroscopy

EIS tests were performed using a superimposed sine wave of amplitude 10mV and a frequency range of 10 KHz to 0.01Hz. The charge transfer resistance (R_{ct}) and double layer capacitance (C_{dl}) were computed using the Z^1 Vs Z^{11} plot. The Nyquist plots are shown in **Figure 8**, and the impedance values are shown in **Table 6**. The table shows that as the inhibitor concentration increases, the charge transfer resistance R_{ct} increases while the double layer capacitance C_{dl} decreases. C_{dl} decreases as the thickness of the electrical double layer increases. The EIS findings corroborated the conclusion that there is a considerable association between corrosion rate and the adsorption structure of the inhibitor layer generated at the metal surface [41].

Atomic Absorption Spectrophotometric Studies (AAS)

The inhibitor efficiency (%) of polyester (PES) and polymer composite (PES-RH) was computed using the percentage of Fe dissolved obtained from AAS and the data shown in **Table 7**. The inhibitor efficiency (%) acquired by this technique was found to be in good accord with that obtained by the traditional weight loss method.

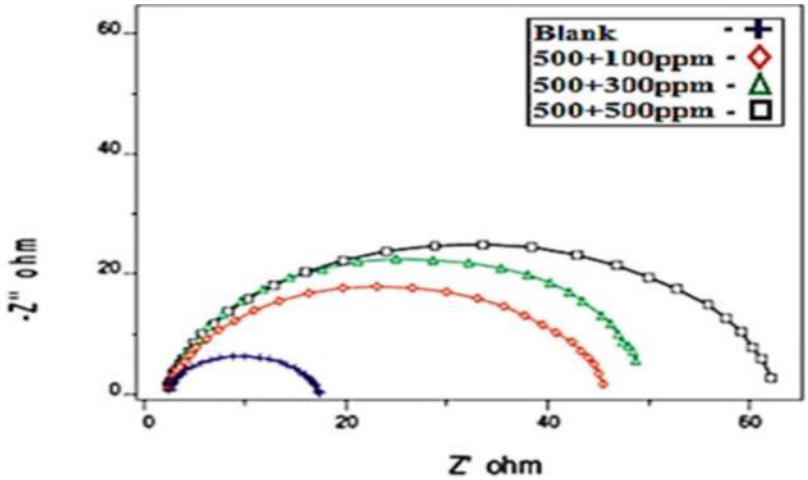

Figure 8 Nyquist diagram for mild steel in 1M H_2SO_4 for selected concentrations of Inhibitor PES-RH

Table 6 AC-impedance parameters for corrosion of mild steel at the inhibitor concentration of polyester / polyester composite in 1M H_2SO_4

Name of the inhibitors	Concentration of PES	Weight of filler materials	R_{ct} (ohm cm^2)	C_{dl} (μF/cm^2)	Inhibition efficiency (%)
Blank	-	-	11.06	27.8	-
PES	500ppm	-	20.8	25.2	46.83
PES-RH	500ppm	RH- 100ppm	36.26	24.8	69.5
		RH- 300ppm	42.54	24.4	74.0
		RH- 500ppm	51.44	23.8	78.5

Table 7 Amount of dissolved iron present in the corrosive solution with and without inhibitors in 1M H_2SO_4 measured using atomic absorption spectrometer

Name of the inhibitors	Concentration of PES	Weight of filler materials	Amount of iron content (mg/l)	Inhibition efficiency (%)
Blank	-	-	1304.96	-
PES	500ppm	-	829.22	36.5
PES-RH	500ppm	RH- 100ppm	307.56	76.4
		RH- 300ppm	165.77	87.3
		RH- 500ppm	157.32	88.0

Atomic force microscopy (AFM) studies

The average roughness, Ra (the average deviation of all points roughness profile from a mean line over the evaluation length), root mean square roughness, Rq (the average of the measured height deviations taken within the evaluation length and measured from the mean line), and maximum peak to valley (P-V) height values were obtained using AFM analysis (largest single peak-to-valley height in five adjoining sampling heights). Rq is far more sensitive than Ra to big and minor height variations from the value for a mild steel surface immersed in acid. The values of Rq, Ra, and P-V height for the surface of mild steel submerged in 1M H_2SO_4 are 226.693 nm, 171.493 nm, and 2023.08 nm, respectively (**Figure 9a** 2D and 3D pictures). The smoothness (non-corroded metal surface) of the surface is due to the creation of a protective film on the metal surface, which inhibits the corrosion of mild steel. The formulation of 500ppm polyester+500ppm rice husk of PES-RH in 1M H_2SO_4 has a Rq value of 195.826 nm, down from 226.693 nm, and an average roughness of 145.705 nm, down from 171.493 nm for a mild steel surface submerged in 1M H_2SO_4. The maximum height from peak to valley is likewise decreased to 1855.73nm. These parameters demonstrate the smoother appearance of the surface [43-47].

Mechanism of inhibition:

Physical or chemical adsorption of inhibitor molecules on the metal surface occurs. Lignin, cellulose, pentosans, carbohydrates, protein, minerals, lipids, and ash are some of the chemical components of rice husk and groundnut shell. Lignin comprises functional groups such as hydroxyl, carboxyl, benzyl alcohol, methoxyl, aldehydic, and phenolic. The functional groups in the natural fillers (rice husk and groundnut shell) aid in the adsorption of the

composite on the mild steel surface by providing a barrier between the metal and the corrodent solution. Furthermore, the presence of primary hydroxyl groups in the chain of cellulose in rice husk improves the composite's adherence to the substrate [42].

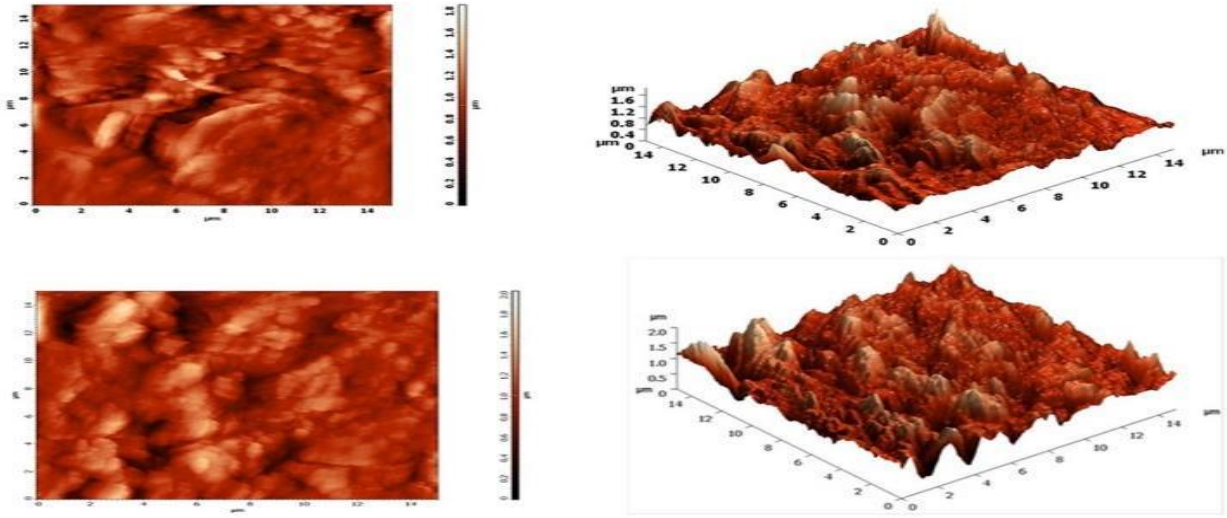

Figure 9 AFM images of a mild steel surface immersed for 3 hours in (a) 1M H_2SO_4 (b) 1M H_2SO_4 + PES-RH

Conclusions

- The PES-RH composite was created by ultrasonically combining RH and PES.
- The use of a polyester composite (PES-RH) to stop mild steel corrosion in an acidic environment proved to be highly successful.
- The inhibitor adsorption on the mild steel surface followed the Langmuir adsorption isotherm.
- The smaller negative value of $\Delta G°_{ads}$ showed that the inhibitors adsorb spontaneously on the metal surface.
- EIS experiments revealed that as the inhibitor concentration was raised, the R_{ct} increased while the C_{dl} dropped due to the increased thickness of the adsorbed layer.
- The Tafel slopes derived from potentiodynamic polarisation curves indicated that all of the inhibitors exhibited mixed behaviour.
- The FT-IR, SEM, EDS, powder XRD, and AFM spectra indicated the development of a protective layer on the surface with mild steel.

Reference

[1] Vinothkumar K, Nivetha M, Sethuraman MG (2020) Robust composite coating with superior corrosion inhibitory performance on surgical grade 316L stainless steel in Ringer solution. Iran Polym J 29:919–931

[2] Hamidi Z, Mosavian SY, Sabbaghi N (2020) Cross-linked poly(N-alkyl-4-vinylpyridinium) iodides as new eco-friendly inhibitors for corrosion study of St-37 steel in 1 M H2SO4. Iran Polym J 29:225–239

[3] Pekdemir ME, Öner E, Kök M (2021) Thermal behavior and shape memory properties of PCL blends film with PVC and PMMA polymers. Iran Polym J 30: 633–641

[4] Dagdag O, El Harfi A, El Gana L, Hlimi Z, Erramli H, Hamed O, Jodeh S (2019) The role of zinc phosphate pigment in the anticorrosion properties of bisphenol a diglycidyl ether-polyaminoamide coating for aluminum alloy AA2024-T3. J Bio-Tribo-Corros 5(1):7-16

[5] Huang R, Guo X, Ma S, Xie J, Xu J, Ma J (2020) Novel phosphorus-nitrogen-containing ionic liquid modified metal-organic framework as an effective flame retardant for epoxy resin. Polymers 12(1):108-120

[6] Dagdag O, Hsissou R, Berisha A, Erramli H, Hamed O, Jodeh S, El Harfi A (2019) Polymeric-based epoxy cured with a polyaminoamide as an anticorrosive coating for aluminum 2024–T3 surface: experimental studies supported by computational modeling. J Bio-Tribo-Corros 5:58-64

[7] Levchik GF, Grigoriev YV, Balabanovich AI, Levchik SV, Klatt M (2000) Phosphorus-nitrogen containing fire retardants for poly (butylene terephthalate). Polym Int 49:1095–1100

[8] Jadhav SA, Rane A, Abitha V, Suchithra P, Patil SS, Narute ST (2015) Polymeric particle board: a sustainable substitute to wooden boards. Moroc J Chem 3:2723–2729

[9] Dagdag O, El Bachiri A, Hamed O, Haldhar R, Verma C, Ebenso E, El Gouri M (2021) Dendrimeric epoxy resins based on hexachlorocyclotriphosphazene as a reactive flame retardantpolymeric materials: a review. J Inorg Organomet Polym Mater 3:1–22
[10] Dagdag O, Berisha A, Safi Z, Hamed O, Jodeh S, Verma C, Ebenso E, El Harfi A (2020) DGEBA-polyaminoamide as effective anti-corrosive material for 15CDV6 steel in NaCl medium: computational and experimental studies. J Appl Polym Sci 137:48402-48410
[11] Dagdag O, Essamri A, El Gana L, El Bouchti M, Hamed O, Cherkaoui O, Jodeh S, El Harfi A (2019) Synthesis, characterization and rheological properties of epoxy monomers derived from bifunctional aromatic amines. Polym Bull 76:4399–4413
[12] Dagdag O, El Gana L, Hamed O, Jodeh S, El Harfi A (2019) Anticorrosive formulation based of the epoxy resin-polyaminoamide containing zinc phosphate inhibitive pigment applied on sulfo-tartaric anodized AA 7075–T6 in NaCl medium. J Bio-Tribo-Corros 5:25-32
[13] Bekhta A, Elharfi A (2016) Comparative study of the rheological and thermal properties of the formol phenol novolac epoxy and those of the model resin diglycidylether of bisphenol A (DGEBA). Moroccan J Chem 4:61–67
[14] Li L, Cai Z (2020) Flame-retardant performance of transparent and tensile-strength-enhanced epoxy resins. Polymers 12:317-324
[15] Song K, Wang Y, Ruan F, Liu J, Li N, Li X (2020) Effects of a macromolecule spirocyclic inflatable flame retardant on the thermal and flame retardant properties of epoxy resin. Polymers 12:132-140
[16] Rane AV, Abitha V, Jadhava S (2020) Non-isocyanate polyurethane systems: a review. Moroc J Chem 8:8–4
[17] Amin MA, Abd El-Rehim SS, El-Sherbini EEF, Bayoumi RS (2007) The Inhibition of low carbon steel corrosion in hydrochloric acid solutions by succinic acid: Part I. Weight loss, polarization, EIS, PZC, EDX and SEM studies. Electrochim Acta 52: 3588-3600
[18] Kanojia R, Singh G (2005) An interesting and efficient organic corrosion inhibitor for mild steel in acidic medium. Surface Eng 21(3):180–186
[19] Ferry M, Mohd Noor CW, Gaspersz F, Manuputty (2013) Corrosion performance of mild steel in seawater inhibited by allium CEPA. J.Eng Compute Appl Sci 2: 3-8
[20] Lalitha A, Ramesh S, Rajeswari S (2005) Surface protection of copper in acid medium by azoles and surfactants. Electrochim Acta 51:47-55
[21] Srikanth AP, Sunitha TG, Raman V, Nanjundan S, Rajendran N (2007) Synthesis, characterization and corrosion protection properties of poly(N-(acryloyloxymethyl) benzotriazole-co-glycidyl methacrylate) coatings on mild steel. Mater Chem Phys 103: 241-247
[22] Li W, He Q, Zhang S, Pei C, Hou BJ (2008) Some new triazole derivatives as inhibitors for mild steel corrosion in acidic medium. Appl Electrochem 38:289-295
[23] Sivakumar PR, Srikanth AP (2016) Anticorrosive activity of Santalum Album leaves extract against the corrosion of mild steel in acidic medium. Int J Phy Appli Sci 3 (1):10-20
[24] Sivakumar PR, Karuppusamy M, Perumal S, Elangovan A, Srikanth AP (2015) Corrosion Inhibitive effects of Madhuca Longifolia on mild steel in 1N HCl solution. J Envi Nanotech 4(2):31-36
[25] Karuppusamy M, Sivakumar PR, Perumal S, Elangovan A, Srikanth AP (2015) Mimusops Elengi Linn plant extract as an efficient green corrosion inhibitor for mild steel in acidic environment. J Envi Nanotech 4(2):09-15
[26] Sivakumar PR, Karuppusamy M, Vishalakshi K, Srikanth AP (2016) The inhibition of mild steel corrosion in 1N HCl solution by Melia Azedarach leaves extract. Der Pharma Chem 8(12): 74-83.
[27] Sivakumar PR, Srikanth AP (2016) Inhibiting effect of seeds extract of Pithecellobium Dulce on corrosion of mild steel in 1N HCl medium. Int J Eng Sci and Comp 6(8): 2744-2748
[28] Sivakumar PR, Karuppusamy M, Vishalakshi K, Srikanth AP (2016) The inhibition of mild steel corrosion in 1N HCl solution by Melia Azedarach leaves extract. Der Pharma Chemi 8(12):74-83.
[29] Sivakumar PR, Vishalakshi K, Srikanth AP (2016) Inhibitive action of Bombax Malabricum leaves extract on the corrosion of mild steel in 1N HCl Medium. J Appli Chemi 5(5):1080-1088
[30] Vishalakshi K, Sivakumar PR, Srikanth AP (2016) Tetrameles Nudiflora Leaves Extract as Green Corrosion Inhibitor for Mild steel in Hydrochloric Acid Solution. Int Org Sci Res J Appl Chemi 9(9):50-55
[31] Sivakumar PR Srikanth AP (2016) Inhibiting effect of fruits extract of Santalum Album on corrosion of mild steel in Hydrochloric acid solution. Int Org Sci Res J Appl Chemis 369(10): 29-37
[32] Sivakumar PR, Srikanth AP (2016) Inhibitive action of aqueous extract of Holoptelea integrifolia leaves for the corrosion of mild steel in 1N HCl solution. Der Phar Chemi 8(19):433-440
[33] Sivakumar PR, Karuppusamy M, Vishalakshi K, Srikanth AP (2017) Inhibitory effect of Michelia Champaca

leaves extracts on the corrosion of mild steel in 1N HCl acid: A Green Approach. IOSRD Int J Chemi 4(1):14-18
[34] Sivakumar PR, Srikanth AP (2017) Anticorrosive Activity of Schereabera sweietenoids Leaves as Green Inhibitor for Mild Steel in Acidic Solution. Asian J Chemi 29(2):274-278
[35] Vishalakshi K, Sivakumar PR, Srikanth AP (2016) Analysis of Corrosion Resistance behavior of green inhibitors on mild steel in 1N HCl medium using electrochemical techniques. Der Pharma Chemica, 8(19), 548-553
[36] Sivakumar PR, Srikanth AP (2017) Ziziphus jujube leaves extract as green corrosion inhibitor for mild steel in 1N hydrochloric acid Medium. J Appli Chemis 6(4):476-483
[37] Sivakumar PR, Srikanth AP (2018) Eco friendly green inhibitor for corrosion of mild steel in 1N hydrochloric acid Medium. J Appli Chemis 7(1):239-249
[38] Sivakumar PR, Srikanth AP (2018) Gloriosa superba linn extract as ecofriendly inhibitor for mild steel in acid medium: A comparative study. Asi J Chemis 30(3):513-519
[39] Sivakumar PR, Srikanth AP, Muthumanikam S (2017) The corrosion inhibition and adsorption properties of ecofriendly green inhibitor - A comparative study. Int J Chemtech Res 10(12):386-398
[40] Sivakumar PR, Karuppusamy M, Srikanth AP (2017) Corrosion inhibition of mild steel in 1N HCl media using Millingtonia Hortensis leaves extract. Int Org Sci Res J Appl Chemi 10:65-70
[41] Sivakumar PR, Karuppusamy M, Srikanth AP (2018) Pithecellobium dulce extracts as corrosion inhibitor for mild steel in acid medium. Der Pharma Chemi 10:22-28
[42] Sivakumar PR and Srikanth AP (2020) Green corrosion inhibitor: A comparative study. Sadhana 45:45-56
[43] Velayutham Rajeswari, Devarayan Kesavan, Mayakrishnan Gopiraman, Periasamy Viswanathamurthi, Kaliyaperumal Poonkuzhali, Thayumanavan Palvannan. Corrosion inhibition of Eleusine acgyptiaca and croton rottlerin leaf extract on cast iron surface in 1M HCl medium, Applied Surface Science, 2014 314, 537-545
[44] Sakunthala P, Charles A, Kesevan D, Alex Ramani V Phytochemical screening and adsorption studies of brugamanisa suaveolens. Chemical Science Review and Letters 2014, 2, 319-322.
[45] Rajeshwari V, Devarayan K, Mayakrishanan G, Viswanathamurthi P. Inhibition of cast iron corrosion in acid, base and netural media using Schiff base derivatives, Journal of Surfactant and Detergents 2013, 16, 571-580.
[46] Vivekananthan Shanmuga Sundaram, Sakunthala Pitchai, Kesavan Devarayan, Gopiraman Mayakrishnan, Alexramani Vincent, and Sulochana Nagarajan Devarayan K Effect of green inhibitor on acid corrosion of A2S1 1022 steel. Chemical Science Review and Letters 2013, 1, 195-200.
[47] Muthu Nadar Lavanya, Devarayan Kesavan, Nagarajan Prabhavathi and Nagarajan Sulochana, Studies on the inhibitive effect of 3-hydroxy flavone on acid corrosion of mild steel surface. Chemical Science Review and Letters 2009, 16(6), 845-853.

Publication History
Received 30.10.2021
Revised 04.02.2022
Accepted 06.02.2022
Online 31.03.2022